International Journal of Modern Physics B
Vol. 31 (2017) 1744034 (7 pages)

DOI: 10.1142/S0217979217440349

Prediction of corrosion fatigue crack initiation behavior of A7N01P-T4 aluminum alloy welded joints

J. An*, J. Chen*,†, G. Gou*,§, H. Chen* and W. Wang‡

*School of Materials Science and Engineering,
Southwest Jiaotong University,
Chengdu 610031, P. R. China

†Chengdu Industry and Trade College,
Chengdu 611731, P. R. China

‡CRRC Qingdao Sifang Co., Ltd.,
Qingdao 266000, P. R. China

§gouguoqing1001@163.com

Received 13 October 2016
Published 5 May 2017

Through investigating the corrosion fatigue crack initiation behavior of A7N01P-T4 aluminum alloy welded joints in 3.5 wt.% NaCl solution, corrosion fatigue crack initiation life is formulated as $N_i = 6.97 \times 10^{12}[\Delta\sigma_{\text{eqv}}^{1.739} - 49^{1.739}]^{-2}$ and the mechanism of corrosion fatigue crack initiation is proposed. SEM and TEM tests revealed that several corrosion fatigue cracks formed asynchronously and the first crack does not necessarily develop into the leading crack. The uneven reticular dislocations produced by fatigue loading are prone to piling up and tangling near the grain boundaries or the second phases and form the "high dislocation-density region" (HDDR), which acts as an anode in microbatteries and dissolved to form small crack. Thus the etching pits, HDDR near the grain boundaries and second phases are confirmed as the main causes inducing the initiation of fatigue crack.

Keywords: A7N01P-T4 Al alloys; corrosion; crack initiation; fatigue life prediction.

1. Introduction

Aluminum (Al) is prone to pitting corrosion in chloride-containing environments as quarter-elliptical corner cracks tend to initiate at the edge of notch.[1] The formation of pits is attributed to the chemical or physical heterogeneity at the surface, such as inclusions, second-phase particles and flaws.[2,3] Zhang *et al.* studied the electrochemical local corrosion behavior of 7A52 Al alloy and found that the preferential dissolution of Mg_2Si was the main reason leading to the development of

§Corresponding author.

corrosion pits.[4] Previous studies revealed that pits nucleation occurred at the microscopic level with some metals displaying preferential sites for pit nucleation.[5] The crystalline defects including twins and dislocations resulting from severe plastic deformation weakened the corrosion resistance of Mg and its alloys.[6,7] A great deal of works has identified dislocation channeling as a potential factor controlling stress corrosion cracks.[8,9]

In this paper, the effect of pits and dislocation on corrosion fatigue crack initiation of A7N01P-T4 Al alloy welded joints in 3.5 wt.% NaCl solution was investigated; and the mechanism of corrosion fatigue crack initiation was discussed.

2. Materials and Experimental Techniques

The chemical compositions of Al alloy and welding wire are listed in Table 1 and the welding parameters are listed in Table 2. Figure 1 shows the details of the test specimen.

2.1. *Materials*

2.2. *Corrosion fatigue crack initiation experiment test*

An 810 Material Test System low-frequency fatigue test machine was used in fatigue test and the specimens were loaded with the stress ratios $R = 0.4$, 0.5, 0.6 and 0.7

Table 1. Chemical compositions of A7N01P-T4 aluminum alloy and welding wire.

Material	Zn	Mg	Cu	Mn	Ti	Si	Fe	Cr	Al
A7N01P-T4	4.0–5.0	1.0–1.8	0.10	0.20–0.70	0.01–0.06	0.35	0.4	0.06–0.2	Bal.
ER5356	0.10	4.5–5.5	0.1	0.05–0.20	0.2	0.25	0.1	—	Bal.

Table 2. Welding parameters for the A7N01P-T4 aluminum alloy welded joints.

Material	Thickness (mm)	Peak current (A)	Welding voltage (V)	Wire feeding speed (m/min)	Welding speed (mm/s)	Laser power (kW)
A7N01P-T4	8	221	25.7	14	8.5	3.2

Note: The gas used for welding is 99.999% purity argon.

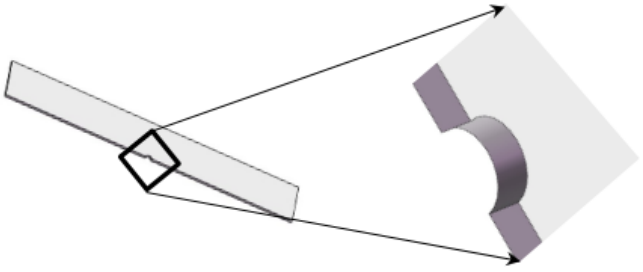

Fig. 1. Corrosion fatigue crack initiation specimen with a semicircular notch.

at a frequency of 5 Hz. Previous reports[6,8] recommended 250 μm as a critical value of fatigue crack initiation.

2.3. *Microstructure observation*

After the corrosion fatigue crack initiation test, the surface morphology near the semicircular notch was observed by SEM (JSM-6490LV QUANTA FEG 250), electron back-scattered diffraction (EBSD) and TEM (JEM-2100F).

3. Results and Discussion

3.1. *Prediction of corrosion fatigue crack initial life*

Figure 2 shows the corrosion fatigue crack initiation curves of crack length versus number of cycles. The stress ratio R increased from 0.4 to 0.7, the number of cyclic loadings subsequently descended from 1.118×10^6 to 6.214×10^4 when a crack of 250 μm length is generated.

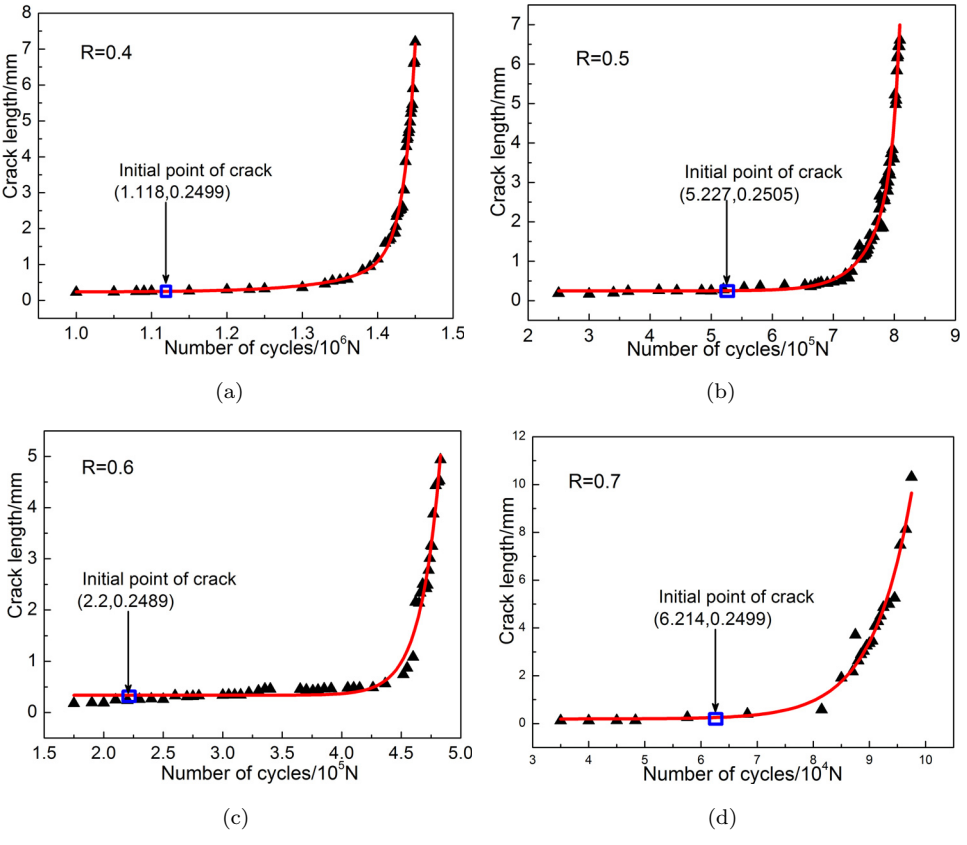

Fig. 2. (Color online) Corrosion fatigue crack initiation curves: (a) $R = 0.4$, (b) $R = 0.5$, (c) $R = 0.6$, (d) $R = 0.7$.

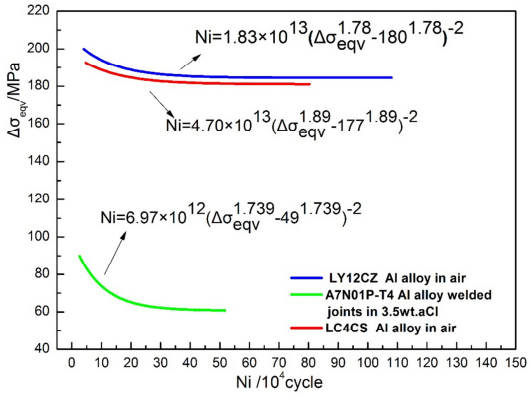

Fig. 3. (Color online) Fatigue crack initiation life curves in air and 3.5 wt.% NaCl solution.

In previous study, fatigue life curve has been described as $N_i = C_{\text{icf}}[\Delta\sigma_{\text{eqv}}^{2/(1+n)} - (\Delta\sigma_{\text{eqv}})_{\text{thcf}}^{2/(1+n)}]^{-2}$. On the basis of calculation, fatigue crack initiation threshold value $(\Delta\sigma_{\text{eqv}})_{\text{thcf}}$ and fatigue crack initiation resistant factor C_{icf} are 49 MPa and 6.97×10^{12}, respectively. So the fatigue crack initiation life curve of A7N01P-T4 welded joints can be described as

$$N_i = 6.97 \times 10^{12}[\Delta\sigma_{\text{eqv}}^{1.739} - 49^{1.739}]^{-2}. \quad (1)$$

Compared with the fatigue crack initiation life of Al alloy in air, corrosion fatigue crack initiation life of Al alloy in NaCl solution was sharply shortened (Fig. 3).

3.2. *Mechanism of corrosion fatigue crack initiation*

Figure 4 showed the process of corrosion fatigue crack initiation. When the number of cycles reached 30,000, two continuous etching pits with a diameter of about 130 μm formed at the edge of semicircular notch [Fig. 4(a)]. When the number of cycles added up to 100,000, two continuous etching pits were connected together and spread into the microcrack 1 [Fig. 4(b)]. When cycles increased to 720,000, another crack 2 appeared analogously at the edge of semicircular notch [Fig. 4(c)]. With the number of cycles increasing further to 800,000, crack 1 ceased propagation at a definite depth. On the contrary, crack 2 propagated continuously and developed into the leading crack [Fig. 4(d)].

After the test, the area near the semicircular notch was observed using SEM [Fig. 5]. Besides crack 1 and crack 2, crack 3 formed at the edge of semicircular notch [Fig. 5(c)], which robustly demonstrates that the multisource close scrutiny reveals that only crack 1 is formed from etching pits.

It has been verified in Fig. 4 that crack 1 was firstly generated during the corrosion fatigue crack initiation but did not end up as the leading crack, which strongly indicates that initial cracks are not always the leading cracks in the ultimate macroscopic perforation failure; and corrosion fatigue cracks do not always initiate from

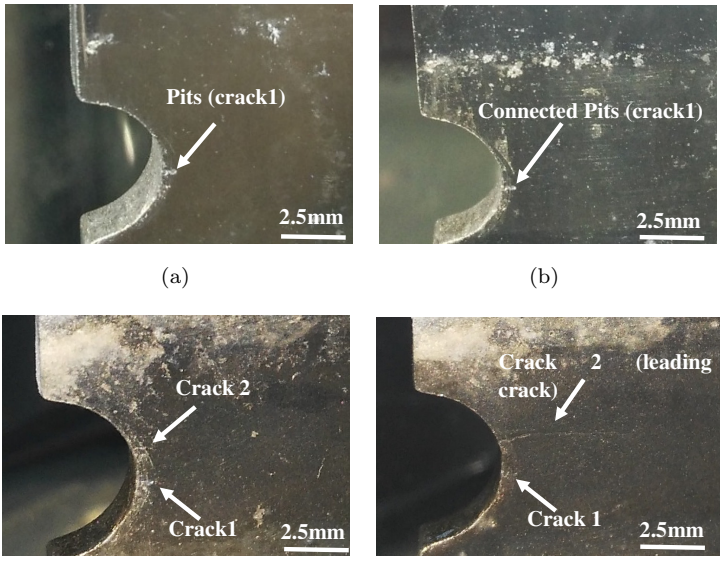

Fig. 4. Macroscopic appearances near the semicircular notch under different cyclic loadings: (a) 30,000 cycles, (b) 100,000 cycles, (c) 720,000 cycles and (d) 800,000 cycles.

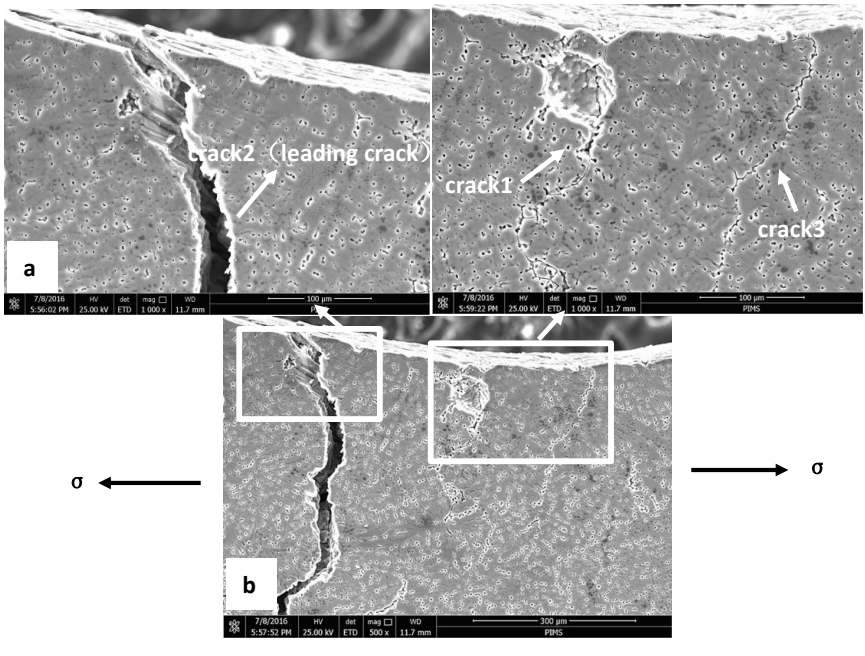

Fig. 5. Microscopic appearances near the semicircular notch: (a) leading crack at high magnification, (b) several crack originals and (c) crack 1 and crack 3 at high magnification.

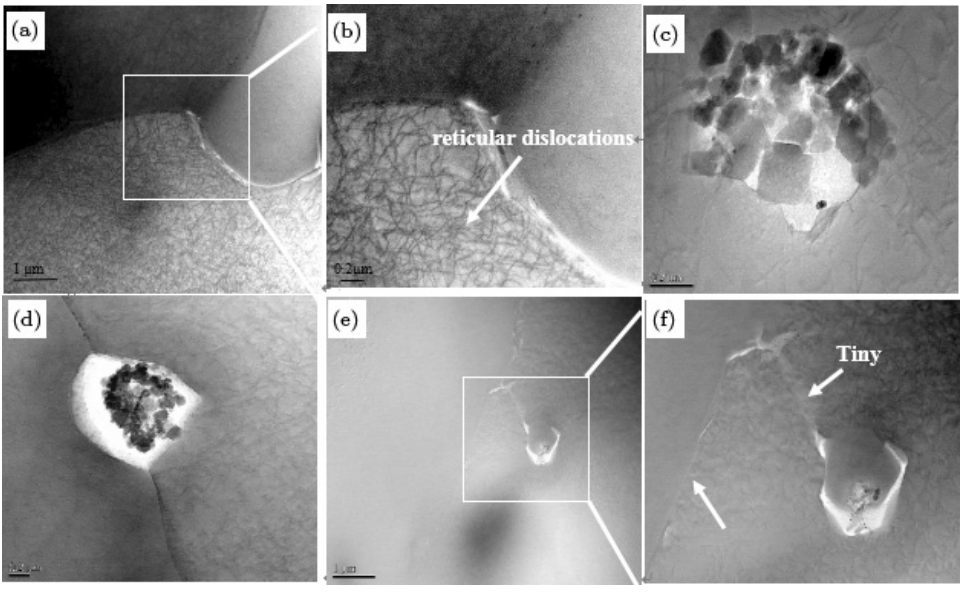

Fig. 6. Dislocations' distributions: (a), (b) near the grain boundaries, (c) near the second-phase particles, (d) near the grain boundary with the second-phase particle and (e), (f) between the grain boundaries and second-phase particle.

etch pits. In Fig. 5(a), the leading crack initially propagated at an angle of about 45° with the loading direction and subsequently deflected in the area 150 μm away from the edge of semicircular notch, propagating on the direction perpendicular to the loading direction. This proves to be the typical fatigue crack initiation by sliding. With the propagation of crack, leading crack gradually moved into the area where more restrictions exist at the plane strain conditions. As a result, the maximum principal stress is in the same direction of loading stress. Thus the leading crack reasonably turns into the direction perpendicular to the loading stress.

After the fatigue loading, micromorphology near the semicircular notch was observed by TEM; and the uneven reticular dislocations were found, which pile up and tangle near the grain boundary to form the "high dislocation-density region" [HDDR; see Figs. 6(a) and 6(b)]. HDDR also lies in the interface of matrix and second phase [Fig. 6(c)]. In particular, when the second phases are located in the grain boundary [Fig. 6(d)] or near the grain boundary [Fig. 6(e)], high dislocation concentration is produced. According to the theory of plastic deformation-activation corrosion, the metal within HDDR is activated. Thus HDDR is most likely to be dissolved and small crack is consequently formed [Fig. 6(f)].

4. Summary

Corrosion fatigue crack initiation behavior of A7N01P-T4 Al alloy welded joints in 3.5 wt.% NaCl solution has been studied; and the following conclusions can be

drawn:

(1) Fatigue crack initiation life of A7N01P-T4 Al alloy welded joints was much shortened in 3.5 wt.% NaCl solution. The fatigue crack initiation life curve of the alloy welded joints could be described as $N_i = 6.97 \times 10^{12}[\Delta\sigma_{\text{eqv}}^{1.739} - 49^{1.739}]^{-2}$.
(2) A large amount of uneven reticular dislocations is formed by the fatigue loading. Reticular dislocations were prone to piling up and tangling near the grain boundaries, forming the HDDR.
(3) HDDRs become the electrochemically active regions and acted as anode in electrolyte, which significantly promoted the initiation of fatigue crack near the grain boundaries and the second phases.

Acknowledgments

The authors acknowledge the financial support from the National Key R&D Program (No. 2016YFB1200602-16).

References

1. H. Jakubczak and G. Glinka, *Int. J. Fatigue* **8**, 57 (1986).
2. R. M. Pidaparti and R. R. Patel, *Mater. Lett.* **62**, 4497 (2008).
3. M. M. Sharma and C. W. Ziemian, *J. Mater. Eng. Perform.* **17**, 870 (2008).
4. P. Zhang, Q. Li and J. Zhao, *J. Shenyang Univ. Technol.* **2**, 32 (2012).
5. G. Burstein *et al.*, *Corros. Eng. Sci. Technol.* **39**, 25 (2004).
6. D. Song *et al.*, *Corros. Sci.* **52**, 481 (2010).
7. D. Song *et al.*, *Corros. Sci.* **53**, 362 (2011).
8. K. Fukuya, *J. Nucl. Sci. Technol.* **50**, 213 (2013).
9. Z. Jiao and G. S. Was, *J. Nucl. Mater.* **408**, 246 (2011).